Supporting information for:

Heteroleptic silver-containing ionic liquids

Neil R. Brooks,[a] Stijn Schaltin,[b] Kristof Van Hecke,[a,c] Luc Van Meervelt,[a] Jan Fransaer[b], Koen Binnemans*[a]

[a] *KU Leuven, Department of Chemistry, Celestijnenlaan 200F - bus 2404, B-3001 Leuven, Belgium; Fax: +3216327992; Tel: +3216327446; E-mail: koen.binnemans@chem.kuleuven.be*
[b] *KU Leuven, Department of Metallurgy and Materials Engineering, Kasteelpark Arenberg 44 - bus 2450, B-3001 Leuven, Belgium; E-mail: jan.fransaer @mtm.kuleuven.be*
[c] *Ghent University, Department of Inorganic and Physical Chemistry, Krijgslaan 281 - S3, B-9000 Gent, Belgium.*

Methods

All chemicals purchased were of reagent grade and used without further purification. [Ag(MeCN)][Tf_2N] was synthesised as previously described [S1]. TGA studies were performed on a TA instruments Q600 thermogravimeter. The temperature was scanned from room temperature up to 400 °C at a heating rate of 5 °C per minute. Elemental analyses (C, H, N) were carried out using a CE Instruments EA-1110 elemental analyser. The IR and Raman spectra were recorded on a Bruker Vertex 70 FTIR spectrometer, coupled with a Ram II Raman module, at a resolution of 4 cm^{-1}. Melting points were determined on a Mettler-Toledo 822 DSC instrument at a heating rate of 10 °C per minute. Viscosities have been measured on a Brookfield cone plate viscosimeter (LVDV-II + Programmable Viscometer) with a cone spindle CPE-40. The ionic liquid was kept under a dry nitrogen atmosphere during the measurement and the temperature of the sample was controlled by a circulating water bath. The morphology and elemental composition of the silver deposits were determined by scanning electron microscopy (SEM) and energy-dispersive X-ray analysis (EDX) (Philips XL 30 FEG) and atomic force microscopy (AFM) (Digital Instruments Nanoscope III AFM).

The electrochemical experiments were performed in an argon filled glove box with O_2 and H_2O concentrations below 1 ppm. Gold-covered silicon wafers have been used as the substrates for electrodeposition. In order to make the current density uniform across the whole electrode area, the electrode was recessed by placing it inside a PTFE-sample holder, which decreased the tendency for dendritic growth. Before use, these substrates were cleaned by rinsing with acetone and dried. After the deposition of a silver layer, they were rinsed with acetone and ethanol and dried. The solution was contained in a platinum crucible and was not stirred during the experiments. The counter-electrode was a silver coil. The experiments were performed using a Solartron instruments SI 1287 electrochemical interface controlled by a computer with CORRWARE software. All potentials in this paper are relative to a silver wire directly immersed in solution (pseudoreference electrode). If required, the potential values were corrected for the iR drop in real time by using the current interrupt technique. During all the electrochemical experiments, the temperature was kept at 90°C.

Synthesis

$[Ag(MeIm)_2][Tf_2N]$: to $[Ag(MeCN)][Tf_2N]$ (4.680 g, 10.9 mmol) was added 1-methylimidazole (2.709 g, 21.8 mmol) in acetonitrile (25 ml) and left to stir for 1 hour. The acetonitrile was removed in vacuo to give $[Ag(MeIm)_2][Tf_2N]$ (6.783g, 10.7 mmol, yield 97.8%) as a white solid. Melting point: 87 °C. Found: C, 30.4 %; N, 10.8%. Calc. For $C_{16}H_{24}AgF_6N_5O_4S_2$: C, 30.2%; N, 11.0%.

$[Ag(BuIm)_2][Tf_2N]$: to $[Ag(MeCN)][Tf_2N]$ (4.680 g, 10.9 mmol) was added 1-butylimidazole (2.709 g, 21.8 mmol) in acetonitrile (25 ml) and left to stir for 1 hour. The acetonitrile was removed in vacuo to give $[Ag(BuIm)_2][Tf_2N]$ (6.783g, 10.7 mmol, yield 97.8%) as a white solid. Melting point: 42 °C. Found: C, 30.4 %; N, 10.8%. Calc. For $C_{16}H_{24}AgF_6N_5O_4S_2$: C, 30.2%; N, 11.0%.

$[Ag(MeIm)(EtIm)][Tf_2N]$: to $[Ag(MeCN)][Tf_2N]$ (7.017 g, 16.4 mmol) was added 1-methylimidazole (1.343 g, 16.4 mmol) and 1-ethylimidazole (1.572 g, 16.4 mmol) in acetonitrile (25 ml) and left to stir for 1 hour. The acetonitrile was removed in vacuo to give $[Ag(MeIm)(EtIm)][Tf_2N]$ (9.152g, 16.2 mmol, yield 98.6%) as a white solid. Melting point: 35 °C. Found: C, 23.7 %; N, 12.2%. Calc. For $C_{11}H_{14}AgF_6N_5O_4S_2$: C, 23.3%; N, 12.4%.

$[Ag(MeIm)(BuIm)][Tf_2N]$: to $[Ag(MeCN)][Tf_2N]$ (5.648 g, 13.2 mmol) was added 1-methylimidazole (1.081 g, 13.2 mmol) and 1-butylimidazole (1.635 g, 13.2 mmol) in acetonitrile (25 ml) and left to stir for 1 hour. The acetonitrile was removed in vacuo to give $[Ag(MeIm)(BuIm)][Tf_2N]$ (7.714g, 13.0 mmol, yield 98.3%) as a white solid. Melting point: 30 °C. Found: C, 26.4 %; N, 11.6%. Calc. For $C_{13}H_{18}AgF_6N_5O_4S_2$: C, 26.3%; N, 11.8%.

[Ag(EtIm)(BuIm)][Tf_2N]: to [Ag(MeCN)][Tf_2N] (9.170 g, 21.4 mmol) was added 1-ethylimidazole (2.055 g, 21.4 mmol) and 1-butylimidazole (2.654 g, 21.4 mmol) in acetonitrile (25 ml) and left to stir for 1 hour. The acetonitrile was removed in vacuo to give [Ag(EtIm)(BuIm)][Tf_2N] (12.868g, 21.2 mmol, yield 98.8%) as a white solid. Melting point: 27 °C. Found: C, 28.1 %; N, 11.3%. Calc. For $C_{14}H_{20}AgF_6N_5O_4S_2$: C, 27.6%; N, 11.5%.

Crystallography

Crystals [Ag($MeIm)_2$][Tf_2N], [Ag($BuIm)_2$][Tf_2N] and [Ag(EtIm)(BuIm)][Tf_2N] suitable for single crystal X-ray diffraction were mounted on a nylon loop attached to a copper pin and placed in the cold N_2 stream on a Bruker SMART 6000 diffractometer at 100(2) K using Cu Kα radiation (λ = 1.54178 Å). Absorption corrections were applied using SADABS [S2]. A crystal of [Ag(MeIm)(BuIm)][Tf_2N] suitable for single crystal X-ray diffraction was mounted with glue on a glass fibre attached to a brass pin and placed on an Agilent Technologies Supernova diffractometer at 298(2) K using Mo Kα radiation (λ = 0.71073 Å). The absorption correction was applied using CrysAlisPro [S3]. All structures were solved using direct methods and refined by the full-matrix least-squares procedure in SHELXL [S4]. H atoms were placed in calculated positions, or for non-disordered CH_3 groups placed based on the difference electron density around the CH_3 group, and refined using a riding model. In the structure of [Ag($MeIm)_2$][Tf_2N] some of the atoms in the Tf_2N anion displayed poor thermal parameters but no overall disorder model could be ascertained so restraints were applied to four atoms (F14, F27, O18 and O19). The Tf_2N anion in the structure of [Ag(MeIm)(BuIm)][Tf_2N] was totally disordered and modeled in the refinement over two positions with restraints on the bond lengths and angles and the thermal parameters; the occupancy of the major disorder part refined to 65.4(3) %. Furthermore there was positional disorder of the methyl and butyl chains with the occupancies fixed to be 50:50 due to the space group symmetry. The Tf_2N anion in the structure of [Ag(EtIm)(BuIm)][Tf_2N] was totally disordered and modeled in the refinement over two positions with restraints on the bond lengths and angles and the thermal parameters; the occupancy of the major disorder part refined to 72.4(9) %. Furthermore the terminal CH_3 group of the butyl chain was disordered and modelled over two positions again with restraints on the bond lengths and angles and the thermal parameters; the occupancy of the major disorder part refined to 71(2) %. A summary of the crystallographic data can be found below and the complete data in the CIF. The program OLEX2 was also used in refinement and making pictures [S5].

Crystal Data for [Ag(MeIm)$_2$][Tf$_2$N]. $C_{10}H_{12}AgF_6N_5O_4S_2$, M =552.24 g mol^{-1}, monoclinic, a = 11.9627(5) Å, b = 9.0478(3) Å, c = 17.1295(8) Å, β = 90.760(2)°, V = 1853.87(13) Å^3, T = 100 K, space group $P2_1/c$ (no. 14), Z = 4, μ(Cu Kα) = 11.676 mm^{-1}, 15161 reflections measured, 3248 unique (R_{int} = 0.0775) which were used in all calculations. The final wR_2 was 0.1292 (all data) and R_1 was 0.0504 (I>2σ (I)).

Crystal Data for [Ag(BuIm)$_2$][Tf$_2$N]. $C_{16}H_{24}AgF_6N_5O_4S_2$, M = 636.39 g mol^{-1}, triclinic, a = 8.9816(7) Å, b = 16.8076(12) Å, c = 18.0174(18) Å, α = 111.575(3)°, β = 90.026(6)°, γ = 97.337(4)°, V = 2505.3(4) Å^3, T = 100, space group P-1 (no. 2), Z = 4, μ(Cu Kα) = 8.728 mm^{-1}, 26010 reflections measured, 9459 unique (R_{int} = 0.0729) which were used in all calculations. The final wR_2 was 0.1077 (all data) and R_1 was 0.0443 (I>2σ(I)).

Crystal Data for [Ag(MeIm)(BuIm)][Tf$_2$N]. $C_{13}H_{18}AgF_6N_5O_4S_2$, M =594.31, monoclinic, a = 14.7961(11) Å, b = 9.0675(6) Å, c = 17.9641(15) Å, β = 109.152(9)°, V = 2276.7(3) Å^3, T = 298 K, space group $P2_1/c$ (no. 14), Z = 4, μ(Mo Kα) = 1.146 mm^{-1}, 18599 reflections measured, 4655 unique (R_{int} = 0.0257) which were used in all calculations. The final wR_2 was 0.1334 (all data) and R_1 was 0.0443 (>2σ(I)).

Crystal Data for [Ag(EtIm)(BuIm)][Tf$_2$N]. $C_{14}H_{20}N_5O_4F_6S_2Ag$, M =608.34, monoclinic, a = 15.2285(9) Å, b = 8.9449(7) Å, c = 18.0327(11) Å, β = 114.034(3)°, V = 2243.4(3) Å^3, T = 100 K, space group $P2_1/c$ (no. 14), Z = 4, μ(Cu Kα) = 9.714 mm^{-1}, 17237 reflections measured, 3946 unique (R_{int} = 0.1059) which were used in all calculations. The final wR_2 was 0.1980 (all data) and R_1 was 0.0678 (>2σ(I)).

References:

[S1] S. Schaltin, N. R. Brooks, L. Stappers, K. Van Hecke, L. Van Meervelt, K. Binnemans and J. Fransaer, *Phys. Chem. Chem. Phys.*, 2012, **14**, 1706.
[S2] SADABS, version 5.0, An empirical absorption correction program from the SAINTPlus NT, Bruker AXS, Madison, USA, 1998.
[S3] Agilent Technologies, (2011), CrysAlisPro Software system, version 1.171.35.19, Agilent Technologies UK Ltd, Oxford, UK.
[S4] SHELXTL, version 5.1, Bruker AXS, Madison, USA, 1998.
[S5] A. V. Dolomanov, L. J. Bourhis, R. J. Gildea, J. A. K. Howard and H. Puschmann, J. *Appl. Crystallogr.*, 2009, **42**, 339.

Figures

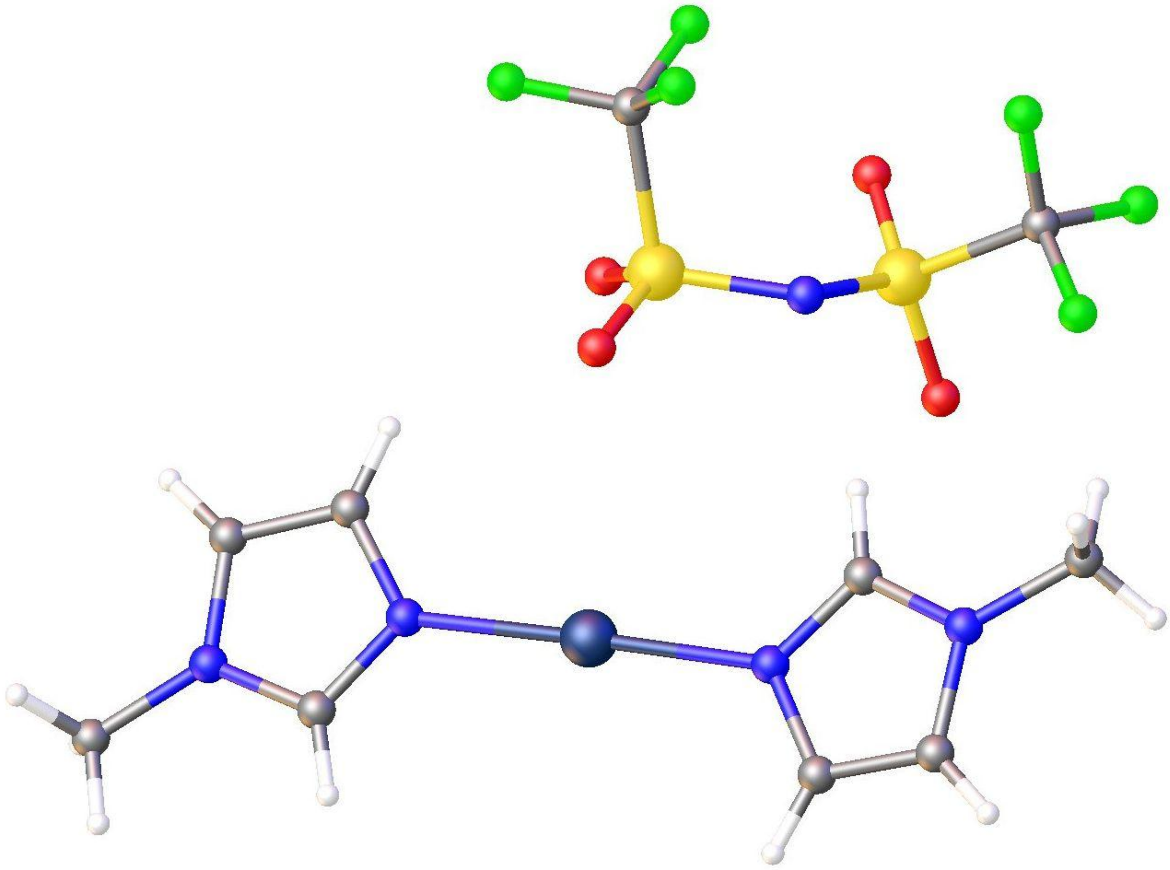

Figure S1: View of the crystal structure of [Ag(MeIm)$_2$][Tf$_2$N] showing the crystallographic asymmetric unit.

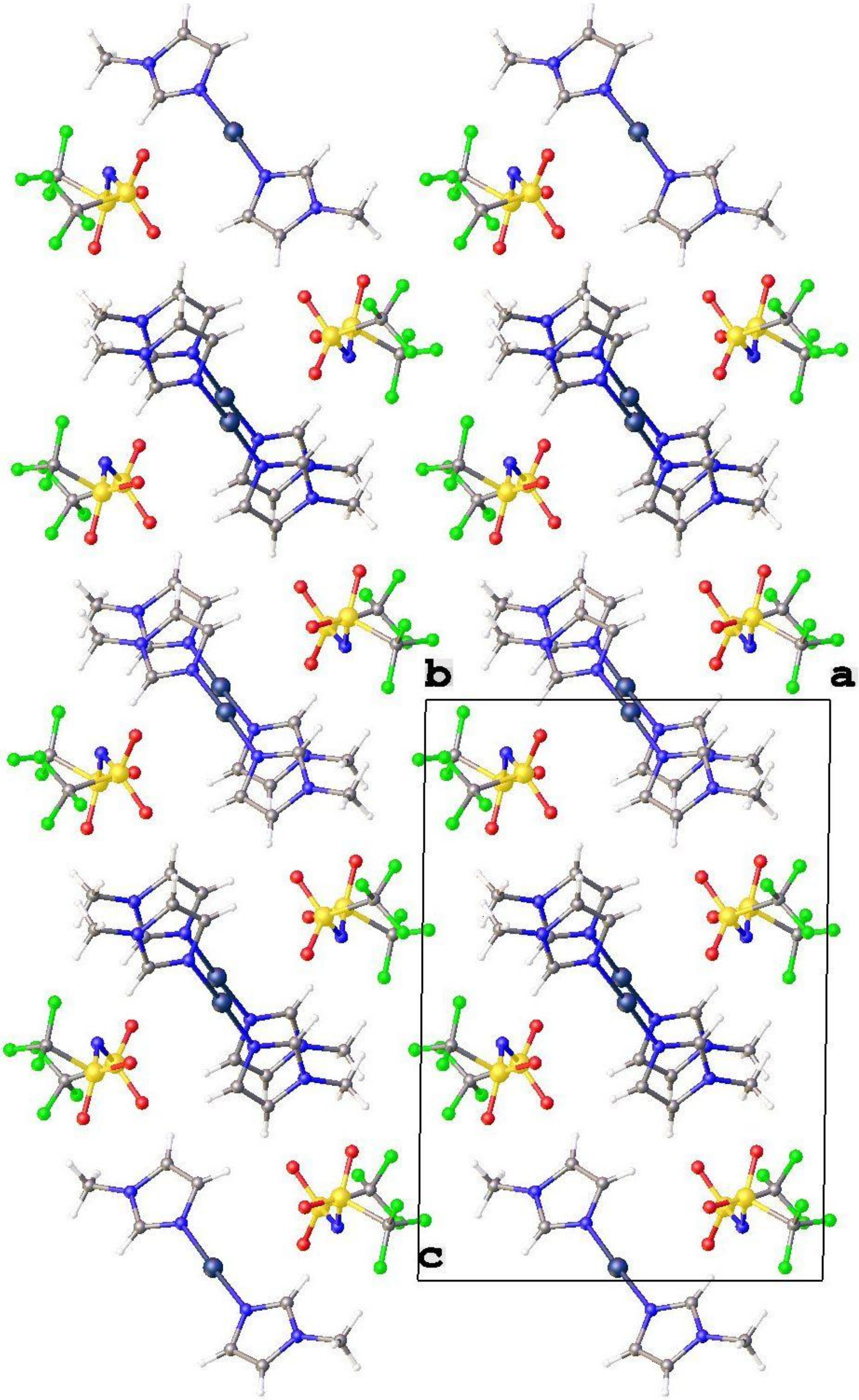

Figure S2: View of the packing in the crystal structure of $[Ag(MeIm)_2][Tf_2N]$.

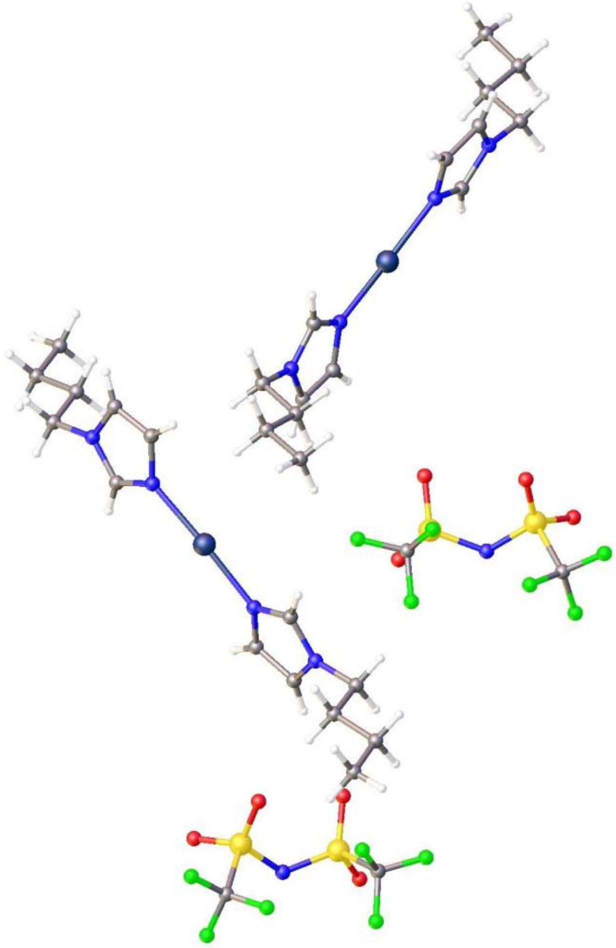

Figure S3: View of the crystal structure of $[Ag(BuIm)_2][Tf_2N]$ showing the crystallographic asymmetric unit.

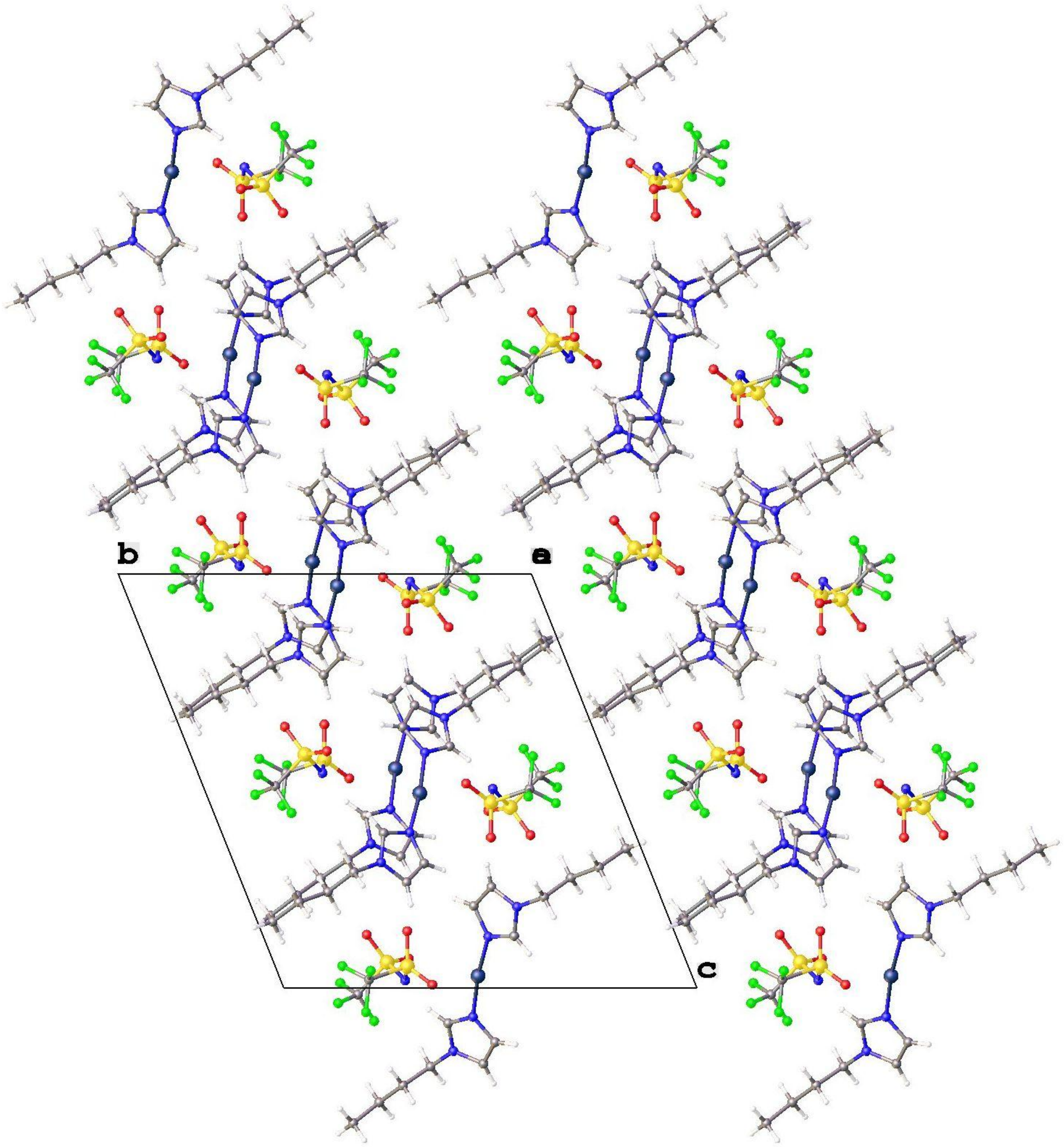

Figure S4: View of the packing in the crystal structure of $[Ag(BuIm)_2][Tf_2N]$.

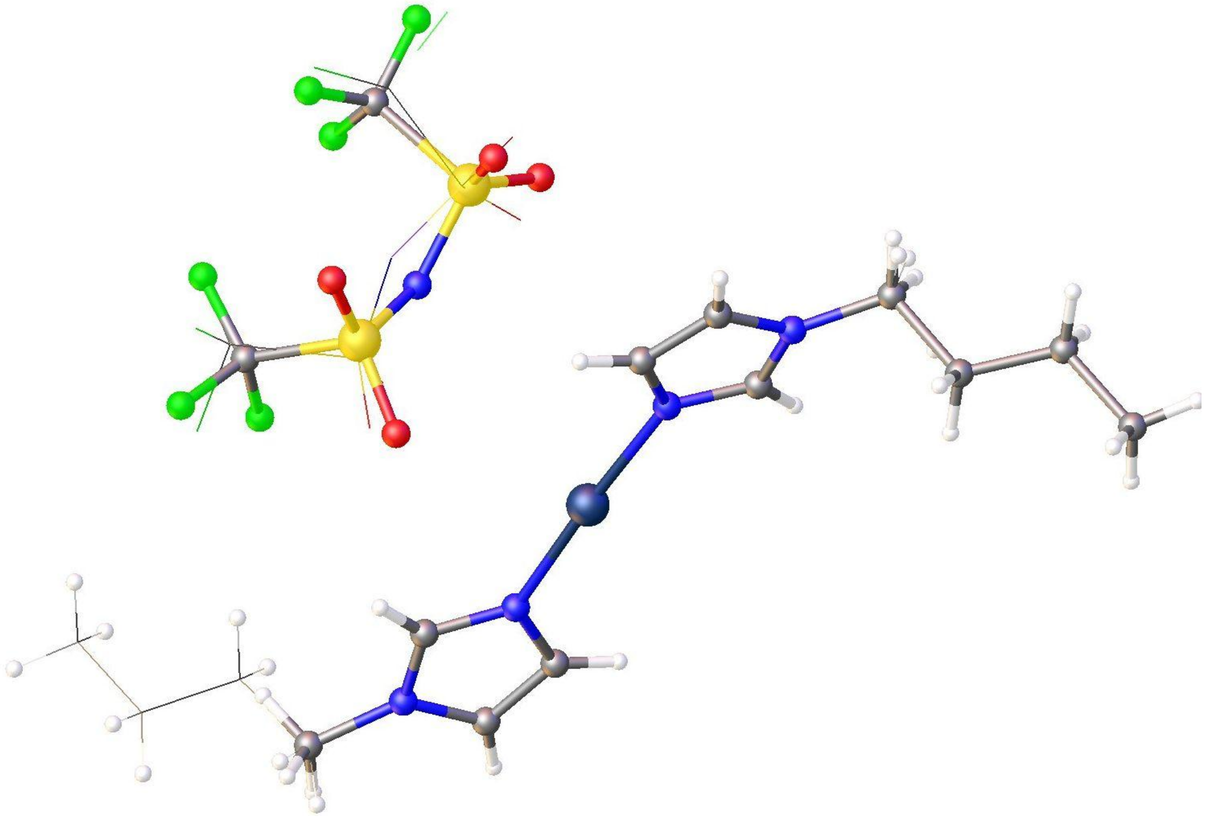

Figure S5: View of the crystal structure of [Ag(MeIm)(BuIm)][Tf_2N] showing the crystallographic asymmetric unit and the disorder of the anion and the butyl chain; one part of the disorder is shown in thick bonds, the other with thin bonds.

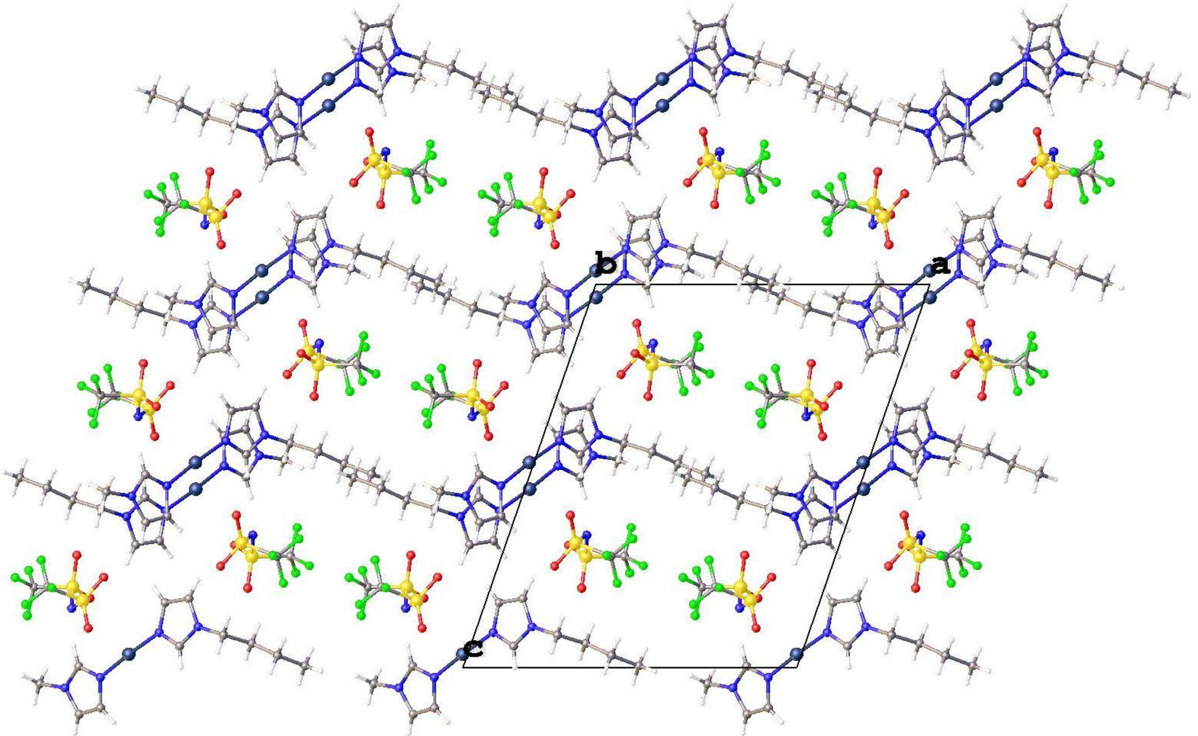

Figure S6: View of the packing in the crystal structure of [Ag(MeIm)(BuIm)][Tf_2N]; disorder omitted for clarity.

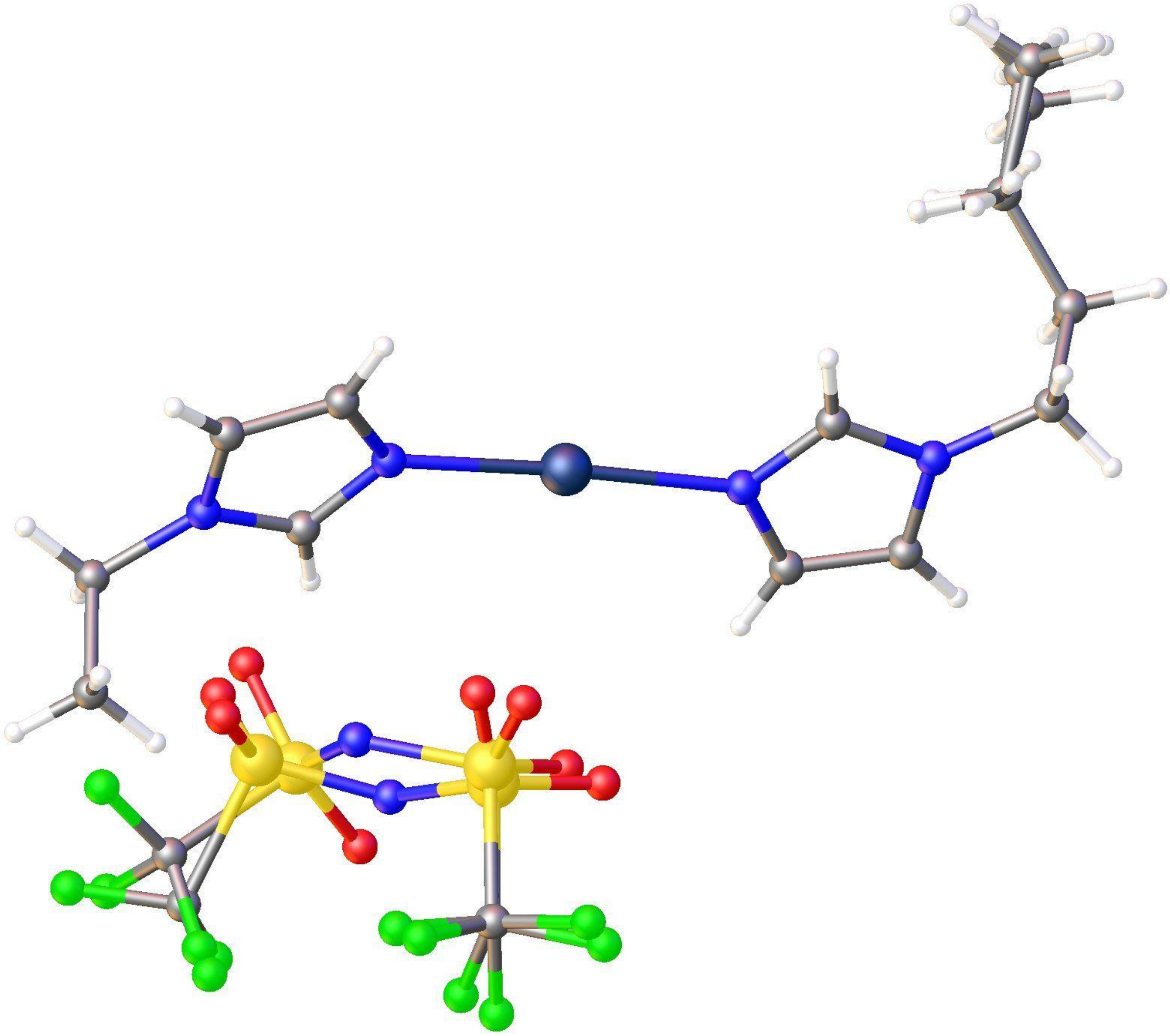

Figure S7: View of the crystal structure of [Ag(EtIm)(BuIm)][Tf_2N] showing the crystallographic asymmetric unit and the disorder of the anion and the butyl chain.

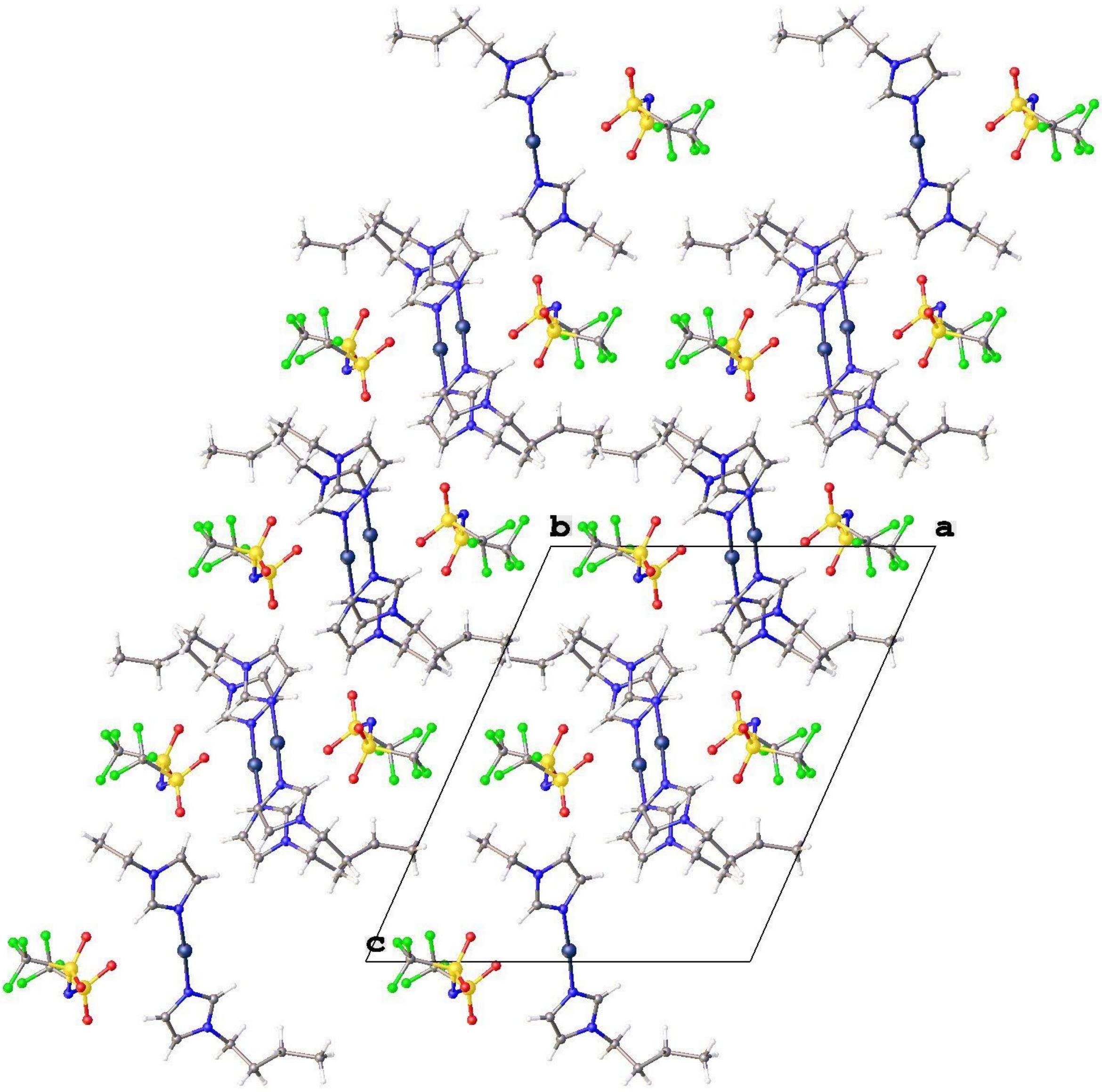

Figure S8: View of the packing in the crystal structure of [Ag(EtIm)(BuIm)][Tf_2N]; disorder omitted for clarity.

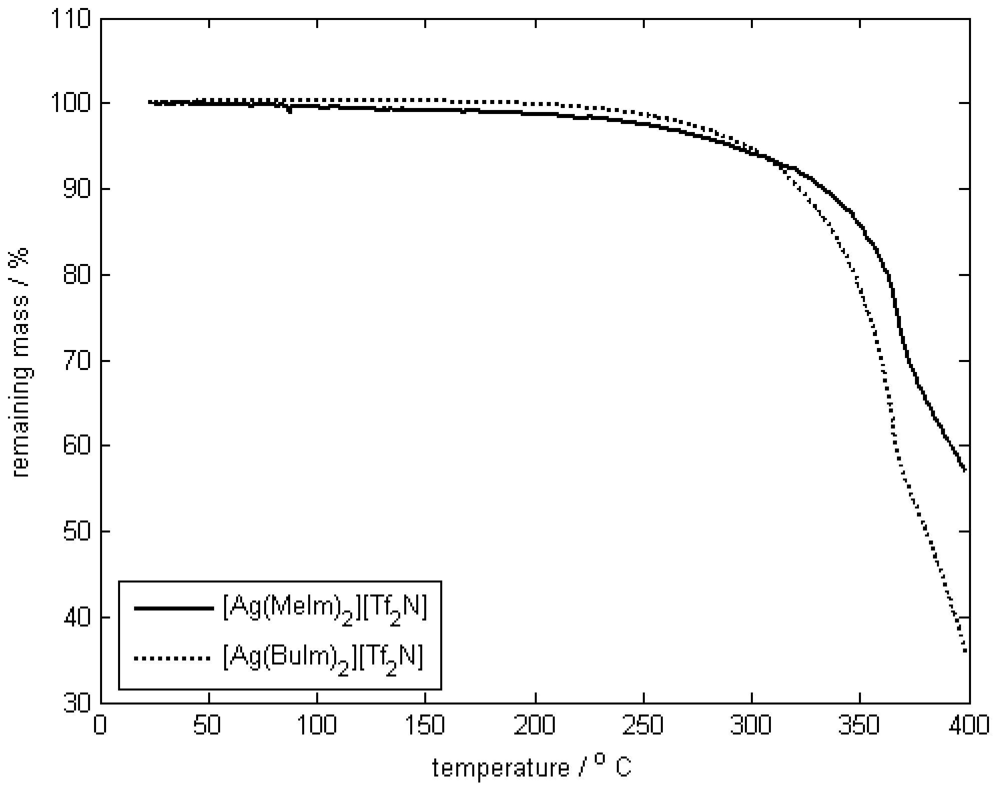

Figure S9: TGA of [Ag(MeIm)$_2$][Tf$_2$N] (solid line) and [Ag(BuIm)$_2$][Tf$_2$N] (dotted line).

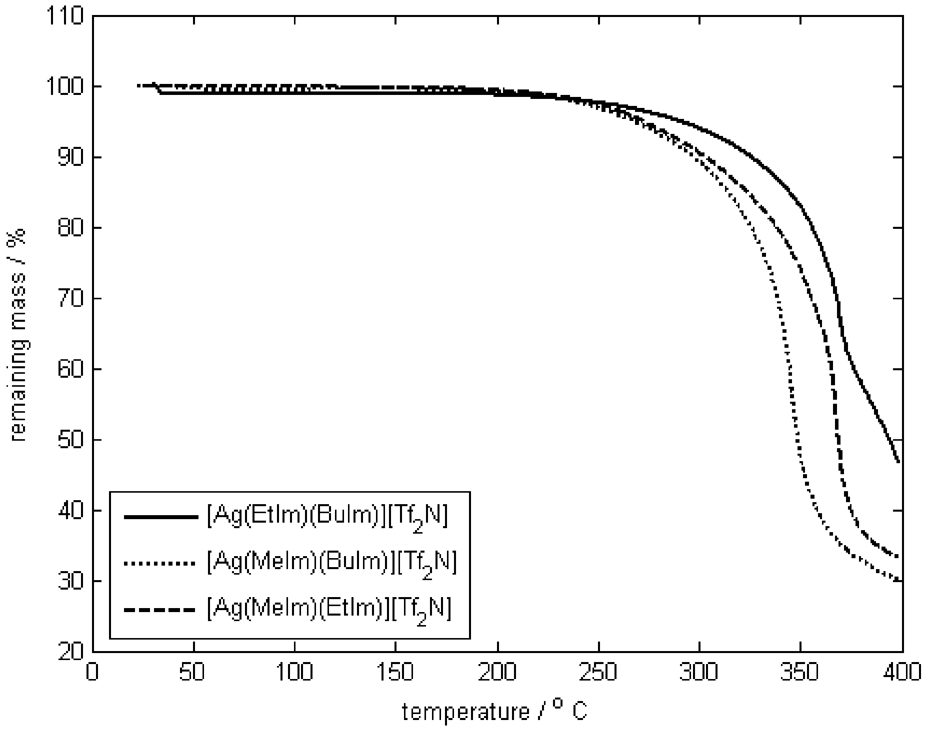

Figure S10: TGA of [Ag(MeIm)(EtIm)][Tf$_2$N] (dashed line), [Ag(MeIm)(BuIm)][Tf$_2$N] (dotted line) and [Ag(EtIm)(BuIm)][Tf$_2$N] (solid line).

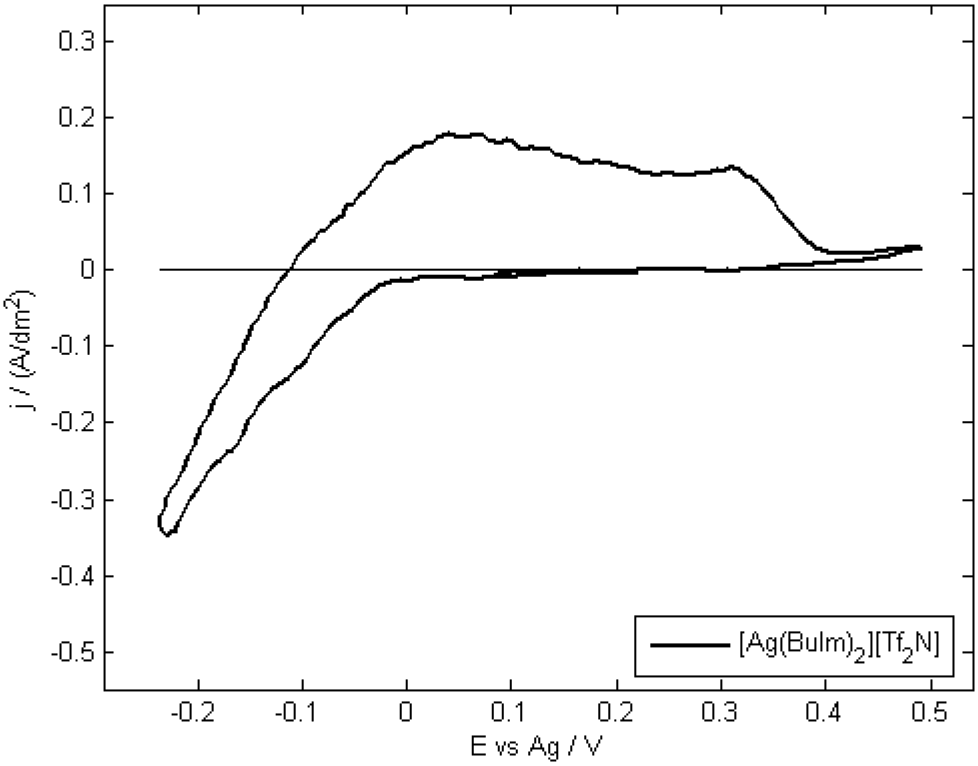

Figure S11: Cyclic voltammogram of [Ag(BuIm)$_2$][Tf$_2$N].

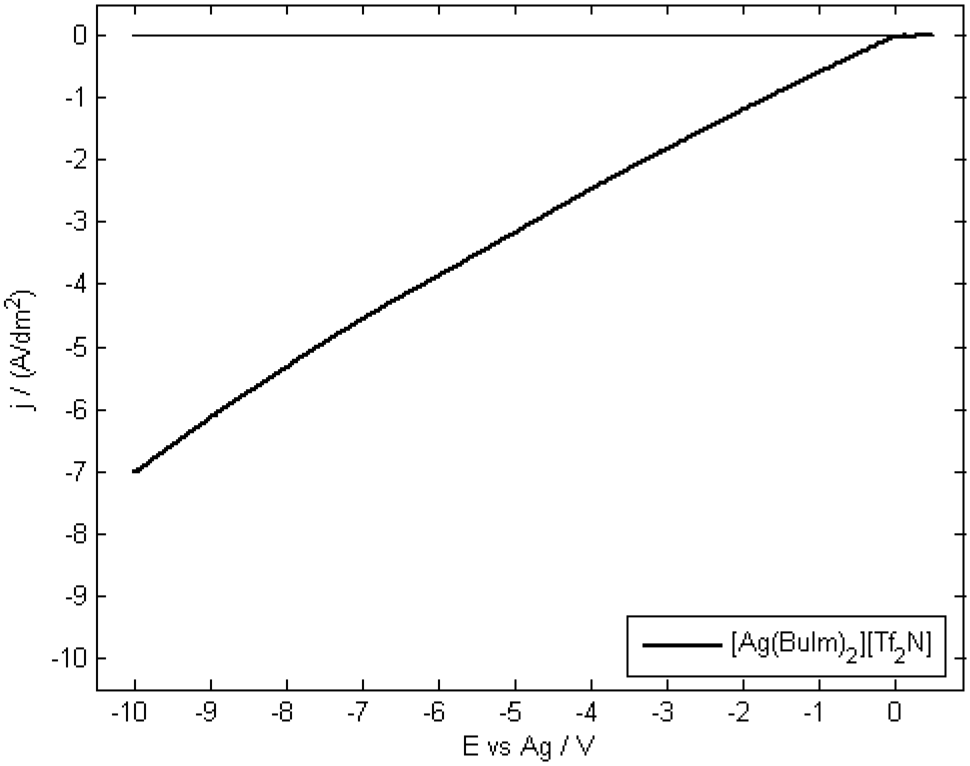

Figure S12: Linear potential scan of [Ag(BuIm)$_2$][Tf$_2$N].

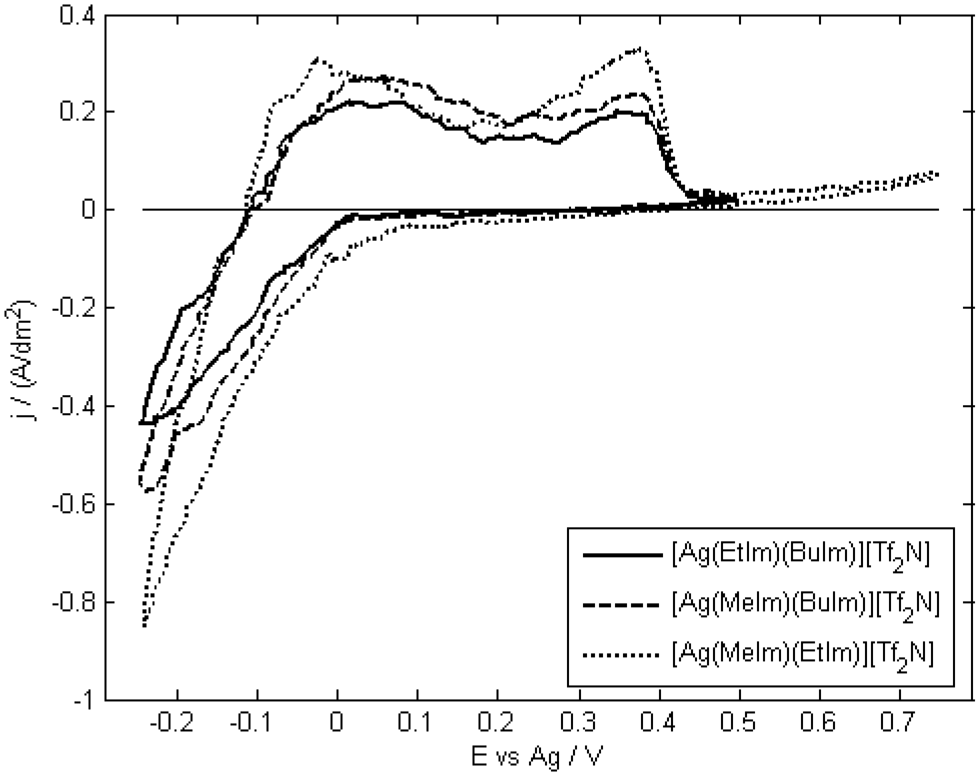

Figure S13: Cyclic voltammogram of [Ag(MeIm)(EtIm)][Tf$_2$N] (dotted line), [Ag(MeIm)(BuIm)][Tf$_2$N] (dashed line) and [Ag(EtIm)(BuIm)][Tf$_2$N] (solid line).

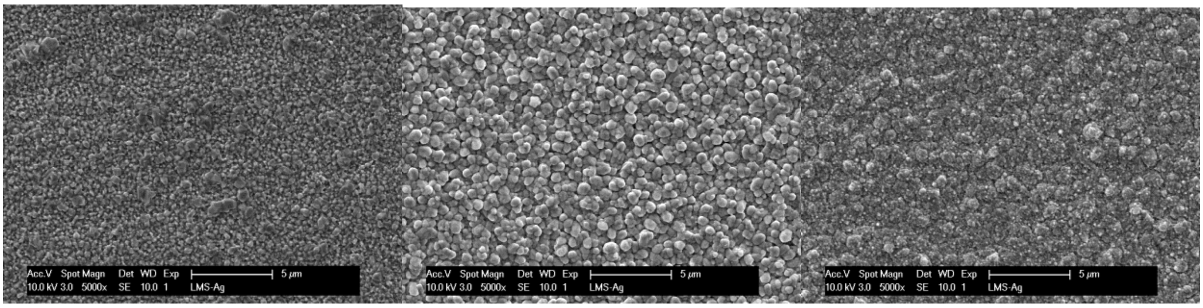

Figure S14: Silver deposits from [Ag(BuIm)$_2$][Tf$_2$N] on an Au working electrode at 90 °C for different current densities: 1 A dm^{-2} (left), 5 A dm^{-2} (centre), and 25 A dm^{-2} (right). The theoretical thickness is 1 µm.

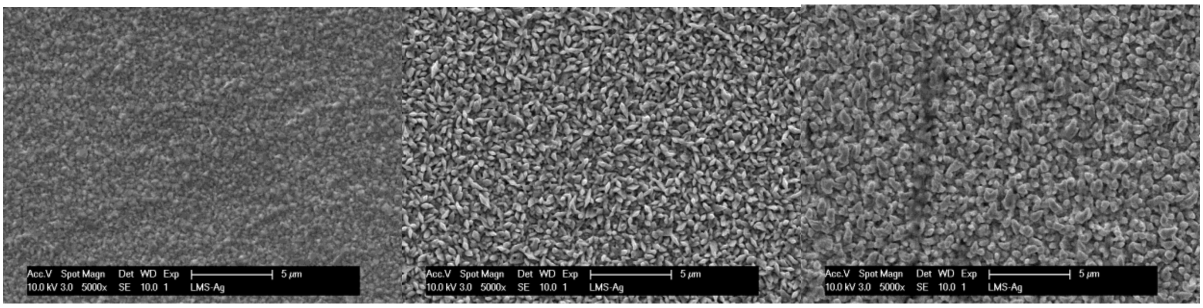

Figure S15: Silver deposits from [Ag(EtIm)(BuIm)][Tf$_2$N] on an Au working electrode at 90 °C for different current densities: 1 A dm^{-2} (left), 5 A dm^{-2} (centre), and 25 A dm^{-2} (right). The theoretical thickness is 1 µm.

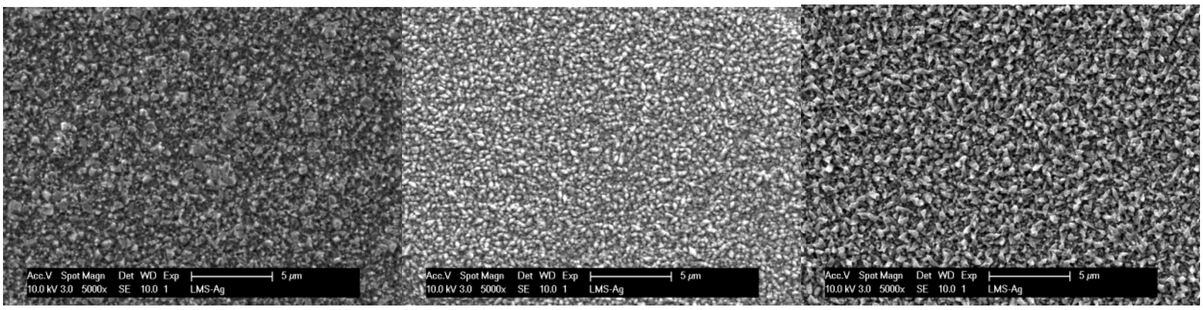

Figure S16: Silver deposits from [Ag(MeIm)(BuIm)][Tf_2N] on an Au working electrode at 90 °C for different current densities: 1 A dm^{-2} (left), 5 A dm^{-2} (centre), and 25 A dm^{-2} (right). The theoretical thickness is 1 µm.

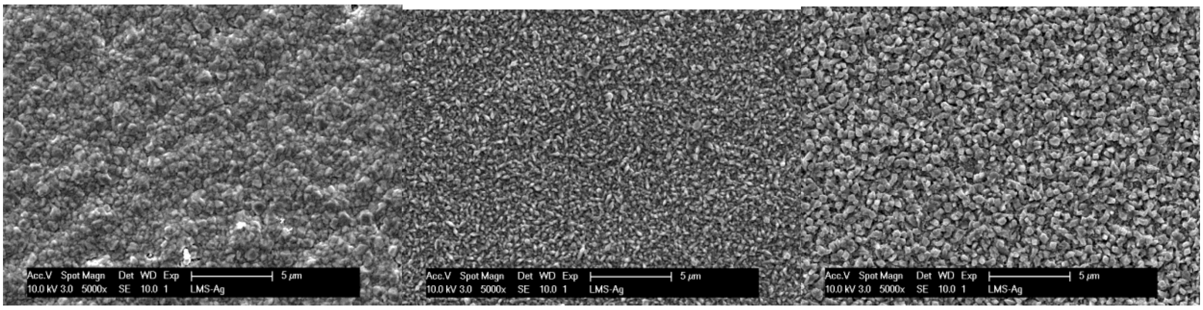

Figure S17: Silver deposits from [Ag(MeIm)(EtIm)][Tf_2N] on an Au working electrode at 90 °C for different current densities: 1 A dm^{-2} (left), 5 A dm^{-2} (centre), and 25 A dm^{-2} (right). The theoretical thickness is 1 µm.